Journal of Hydrology 530 (2015) 273–280

Contents lists available at ScienceDirect

Journal of Hydrology

journal homepage: www.elsevier.com/locate/jhydrol

Glacier mass changes in Rongbuk catchment on Mt. Qomolangma from 1974 to 2006 based on topographic maps and ALOS PRISM data

Qinghua Ye [a,*], Tobias Bolch [b,c], Renji Naruse [d], Yuzhe Wang [e], Jibiao Zong [a], Zhongyan Wang [a], Rui Zhao [a], Daqing Yang [f], Shichang Kang [e,g]

[a] Key Laboratory of Tibetan Environment Changes and Land Surface Processes, Institute of Tibetan Plateau Research, Chinese Academy of Sciences (CAS), Beijing 100101, China
[b] Geographisches Institut, Universität Zürich, 8057 Zürich, Switzerland
[c] Institut für Kartographie, Technische Universität Dresden, 01069 Dresden, Germany
[d] Glacier and Cryospheric Environment Research Laboratory, 2-339, Higashi-machi, Tottori 680-0011, Japan
[e] State Key Laboratory of Cryospheric Sciences, Cold and Arid Regions Environmental and Engineering Research Institute, Chinese Academy of Sciences, Lanzhou 730000, China
[f] National Hydrology Research Center, 11 Innovation Blvd., Saskatoon, Saskatchewan S7N 3H5, Canada
[g] CAS Center for Excellence in Tibetan Plateau Earth Sciences, CAS, Beijing 100101, China

ARTICLE INFO

Article history:
Received 19 November 2014
Received in revised form 8 June 2015
Accepted 5 September 2015
Available online 15 September 2015
This manuscript was handled by Konstantine P. Georgakakos, Editor-in-Chief, with the assistance of Ana P. Barros, Associate Editor

Keywords:
ALOS/PRISM
Digital elevation model (DEM)
Mt. Qomolangma (Mt. Everest MQ)
Rongbuk Catchment (RC)
Glacier mass changes
Topographic maps

ABSTRACT

Elevation changes of glacier surfaces were investigated in Rongbuk Catchment (RC) on the northern slopes of Mt. Qomolangma in the central Himalayas, by comparing a digital elevation model (DEM) generated from the 2006 ALOS/PRISM imageries with the base DEM1974 derived from the 1:50,000 topographic maps. The average elevation change rate of glacier surfaces in RC was estimated at -0.47 ± 0.23 m a^{-1} between 1974 and 2006. Such surface lowering rates varied significantly with glaciers and altitudes. One of the notable results is that the debris-covered ice thinned much more rapidly than the exposed ice at higher altitudes. Overall, glaciers in RC have lost mass of -0.06 ± 0.04 Gt a^{-1} during 1974–2006. Glacier imbalance constitutes about 50% or more of the Rongbuk runoff.

1. Introduction

The Tibetan Plateau (TP) plays an important role in the global climate system and many large rivers originate from this highland region. Glaciers are key components in the TP's cryosphere (Li et al., 2008) and contribute to the local water resources (Immerzeel and Bierkens, 2010). However, the significance of glacier melt water to the overall run-off varies for the different rivers/basins, and knowledge of the relative contribution is still limited (Kaser et al., 2010). In addition, receding glaciers favor the development of supra- and pro-glacial lakes that may cause serious hazards (Fujita et al., 2013). The vast majority of investigated glaciers in TP and in the Himalayas have receded and lost ice mass over the past few decades (Bolch et al., 2012; Yao et al., 2012). However there are local differences, and glaciers with positive mass balances have also been identified, especially in the Karakoram, the western TP and eastern Pamir in recent years (Yao et al., 2012; Gardelle et al., 2013a; Neckel et al., 2014; Kääb et al., 2015).

Glacier variations in TP, China, have been measured by field surveys since the 1950s, and by the use of aerial photographs, topographic maps (the 1970s, 1980s), and remote sensing imageries (mostly Landsat TM/ETM+) since the 1990s (Li et al., 2008; Yao et al., 2012). Using these data, most of the work has focused on changes in glacier areas until now. However, the glacier area changes show signals not only climatic but also non-climatic such as the glacier motion and local topography.

Glacier mass balance indicates the direct response of a glacier to the climate variation. Mass balances can be measured through glaciological, hydrological and geodetic methods. Despite its importance there are only a few records of direct mass balance measurements on Himalayan glaciers (Bolch et al., 2012; Cogley, 2012); e.g. at Glacier AX010 in Nepal (Fujita and Nuimura, 2011), Chhota Shigri

* Corresponding author.
E-mail address: yeqh@itpcas.ac.cn (Q. Ye).

http://dx.doi.org/10.1016/j.jhydrol.2015.09.014
0022-1694/

and Dokriani glaciers in India (Azam et al., 2012; Dobhal et al., 2008) and a few glaciers on TP such as Zha dang, Xiao Dongkemadi, Parlung No. 12/No.94, Qiyi, Kangwure, Gurenhekou, and Naimona'Nyi glaciers glaciers (Ma et al., 2010; Yang et al., 2013; Tian et al., 2014). Difficult accessibility and high labor costs are the major reason that prevents widespread in-situ investigations.

Meanwhile, satellite remote sensing offers a promising opportunity to calculate glacier mass changes through differencing of repeated altimetry profiles or digital terrain models ('the geodetic method'), even in remote mountainous terrains and over several glaciers at a time (Paul and Haeberli, 2008). Geodetic mass balance measurements can also be used for the calibration of direct measurements (Zemp et al., 2013). Recently, several studies of glacier volume/mass changes in High Mountain Asia have been published. Most deal with the Himalayas (Berthier et al., 2007; Gardelle et al., 2013a; Kääb et al., 2015; Vincent et al., 2013); but some are also available for Tibet (Gardner et al., 2013; Neckel et al., 2014). However, these studies focus on the most recent decades since ~2000, and knowledge about mass changes over the earlier periods is still limited. A few long-term geodetic mass balance estimates are for glaciers at Muztag Ata (Holzer et al., 2015), Urumqi Glacier No. 1 (Wang et al., 2014), eastern Himalaya (Racoviteanu et al., 2014), the Aksu-Tarim Catchment (Pieczonka et al., 2013), the Dongkemadi Ice Field (Li et al., 2012), the Purogangri Ice Field (Lei et al., 2012), Laohugou No. 12 glacier (Zhang et al., 2012a,b), and south of Mt. Qomolangma (also known as Mt. Everest, but hereafter only referred to as MQ) for the period 1962–2007 (Bolch et al., 2011).

Hence, the aims of this study are

(a) to calculate glacier mass changes in Rongbuk Catchment (RC, hereafter) of the central Himalaya based on ALOS PRISM DEM and the basic historical DEM, and
(b) to estimate the additional contribution of glacier mass losses to the overall run-off in the catchment.

We have chosen RC on the northern slope of MQ, because of the presence of both clean ice and debris-covered glacier parts, the availability of previous studies to compare with our results, and the existence of relatively long-term climate data in such a remote mountainous region. Our results will also allow a comparison of glacier behaviors between the northern and southern slopes of MQ and a discussion of possible climate controls on glacier changes.

2. Study area

Rongbuk Catchment (RC) covers an area of 280 km^2 ranging from 5120 m to 8844 m a.s.l. (Fig. 1). The mean annual precipitation at the equilibrium line altitude (ELA), situated between 5800 and 6200 m a.s.l., was estimated to range from 500 to 800 mm, and the mean annual temperature to range from −4 to −9 °C (Xie and Su, 1975; Yang et al., 2011). Rongbuk River (RR, hereafter) is mainly fed by Rongbuk Glacier (RG, hereafter), which is the largest glacier in RC and has been fed by three major individual branches: the East, Middle, and West RGs (Fig. 1). All these glacier branches have receded in recent decades, with estimated area losses of 8.9%, 9.4% and 12.2%, respectively during 1974–2008. The total glacier area in RC has decreased by 15 km^2 (or −10.4%) from ~144 km^2 in 1974 to ~129 km^2 in 2008 (Ye et al., 2009). The debris-covered tongues of the three branches had once formed a joint tongue, while they have been separated from each other later. The exact glacier terminus is difficult to locate due to the debris cover (TSETCAS, 1975; Shi and Cheng, 1991). In the debris covered tongue, there is a transition between the active and inactive glacier parts. The thickness of debris cover varies from a few centimeters to several meters. The area of supra-glacial lakes on the debris-covered tongue (Fig. 2) increased from about 0.05 km^2 (16 lakes) in 1974 to about 0.71 km^2 (87 lakes) in 2008 (Ye et al., 2009).

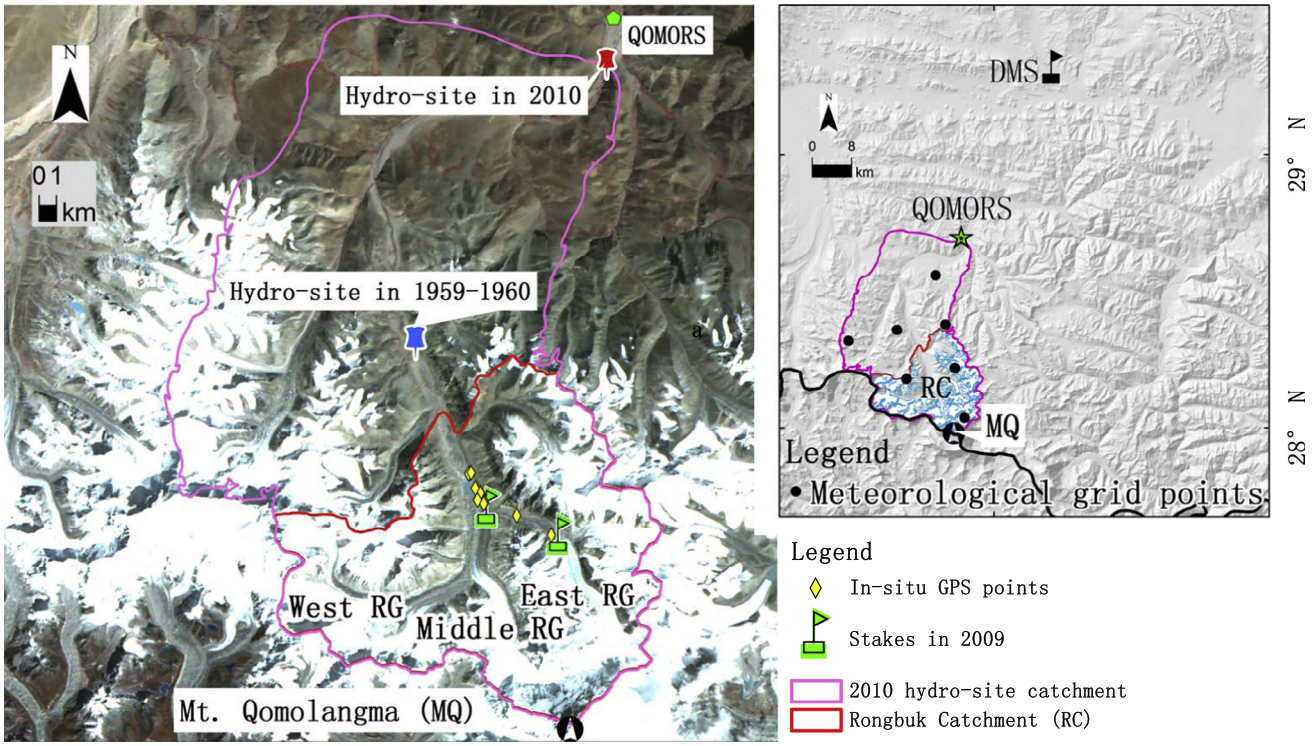

Fig. 1. Mt. Qomolangma region with in-situ GPS points, stakes and hydrological measurement sites in Rongbuk Catchment (RC). The mosaic image shown in this figure is derived from the Chinese satellite HJ1A/1B (http://www.cresda.com/n16/n92006/n92066/n98627/index.html) in October 2012. Inset: Locations of the Dingri meteorological station (DMS), the Qomolangma Atmospheric and Environmental Observation and Research Station, CAS (QOMORS), and meteorological grid points.

3. Data and methods

3.1. Topographic maps and basic elevation data

A digital elevation model of 1974 (DEM1974), was generated by the State Bureau of Surveying and Mapping in China from the digital version of 1:50,000 topographic maps based on aerial photographs acquired in October 1974, with a spatial resolution of 25 m. The original reference system is in the Transverse Mercator projection with the Krasovsky1940 spheroid (Geoid Beijing_1954, Height system Huanghai_1956). The co-registration between DEM1974 and the topographic maps was within a pixel cell and they were used as the common reference system for elevation comparisons in this study. The elevation deviation was compared by 210 evenly distributed spot heights on the topographic maps with the corresponding elevations in the DEM. We obtained an average elevation difference of 0.1 m, with a standard deviation of 8.8 m.

3.2. ALOS PRISM DEM

Three stereo pairs (forward, nadir, backward) of ALOS/PRISM (Advanced Land Observing Satellite/Panchromatic Remote-sensing Instrument for Stereo Mapping) were acquired on 4 December 2006 with a spatial resolution of 2.5 m resolution. Initial DEMs of different resolutions were generated based on the two stereo pairs (i.e., one pair by forward and nadir stereos, the second pair by nadir and backward stereos) using PCI Geomatica Orthoengine, vers. 9.2. The required satellite orbital and altitude variables were obtained from Takeo Tanado from JAXA (Table 1). The same reference system as for the DEM1974 was used, i.e., Transverse Mercator projection and Krasovsky1940 spheroid. We selected 29 Ground Control Points (GCPs) and 12 Tie Points (TPs) from the 1:50,000 topographic maps with the DEM1974 as vertical reference. The identification is challenging in complex mountain topography. We chose points along the mountain range, at peaks and rocks at different altitudes.

The resulting DEMs contained data gaps in some areas where saturation existed, with very low contrast such as shadowed or snow-covered areas. Hence, multiple parameter settings were tested to improve the results. The optimal DEM was obtained with a sampling interval of two grid cells (resolution: 5 m) and an output resolution of 25 m. This matches the spatial resolution of the base DEM1974 and offers a compromise between minimizing data gaps (around 25% on glaciers) and obtaining a fine output resolution. Co-registration to DEM1974 was carried out by shifts ($dx = 65$ m, $dy = 15$ m) that were calculated from a relationship between elevation difference (dh) and terrain factors, i.e. terrain slope (α), terrain aspect (ψ) in ice-free areas according to Nuth and Kääb (2011). The generated DEM was iteratively shifted until the improvement of the standard deviation less than 2%, the final co-registered DEM was named PRISMV06, hereafter.

The final ALOS/PRISM DEM_25m (hereafter PRISM2006; Fig. 3a) was obtained by filling data gaps for PRISMV06 based on a TIN-based delta surface approach (Luedeling et al., 2007) using the ASTER GDEM version 2. The ASTER GDEM2 was transformed into the same projection and datum system as the DEM1974 and resampled to the same spatial resolution of 25 m using bilinear interpolation. In ice free areas, co-registration between DEMs was also carried out by a shifting vector ($dx = 32$ m, $dy = 19$ m) following the method from Nuth and Kääb (2011), while elevation shift was calculated based on the relationship between the elevation difference (Δh_a = ASTER GDEM2 – DEM1974) and the maximum curvature of DEM1974 (x), i.e. $\Delta h_a = 1.68x^3 - 14.53x^2 - 3.17x - 7.68$ ($R^2 = 0.80$), as illustrated by Gardelle et al. (2013b). For the corrected ASTER GDEM2, with respect to the PRISM2006, the average difference was 1.44 m with a standard deviation of 6.06 m. The co-registered PRISM DEMs were evaluated in the ice-free areas with respect to the DEM1974 (Table 2).

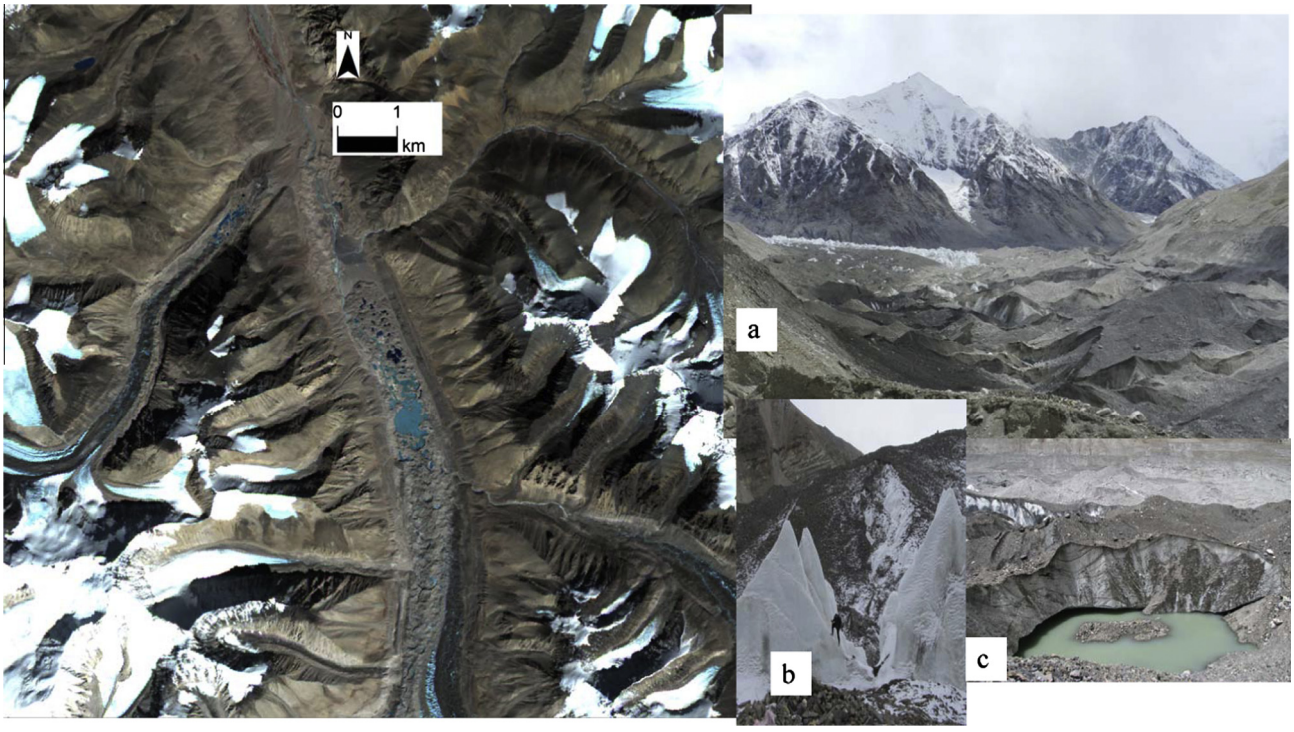

Fig. 2. The debris-covered tongue with supra-lakes around 5200–5800 m of the Middle Rongbuk Glaciers (by ALOS/AVNIR-2 on 24 October 2008, RGB:432). (a) Séracs and the debris-covered tongue; (b) séracs; (c) supra-glacial lake (in-situ photos taken by Q. Ye in September 2011).

Table 1
The parameters of importing ALOS/PRISM into PCI software.

	Backward	Nadir	Forward
Across angle	1.09	1.2	1.09
Along angle	−23.8	0	23.8
Altitude	691,650 m		
IFOV	0.00000361		
Semi-minor	6,356,752 m		
Inclination	98.176		
Ellipsoid	GRS80		
Period	98.7 min		

3.3. Calculation of glacier mass changes

From the difference in surface elevations of glaciers between 1974 and 2006, namely Δh = PRISM2006 − DEM1974, we obtain surface elevation change from 1974 to 2006, whose average annual rate is called simply 'elevation change' (m a^{-1}) hereafter. Grid cells with elevation differences exceeding ±100 m were omitted as outliers (cf. Berthier et al., 2010; Bolch et al., 2011).

Glacier elevation change was obtained as an average in each 20 m altitude interval, distinguishing exposed ice (i.e. clean ice without debris-cover, including ice cliff or séracs) from debris-covered ice areas. Based on previous delineations of 74 segments of glaciers in RC from the topographic maps in 1974 (Ye et al., 2009), the average elevation changes for the exposed ice were also obtained.

Then, the volume change (δV) at each 20 m altitude interval was calculated from the average elevation changes ($\Delta h = dh/dt$) multiplied by the corresponding glacier area in 1974. Values of δV at different altitudes were summed up to give the total volume change (ΔV) in RC. To convert the volume change to mass change, an average glacier density ρ = 850 ± 60 kg m^{-3} was assumed (Huss, 2013). This value is within the range of in-situ measurements at RGs which revealed the density of snow/firn/ice to be between 700 kg m^{-3} and 900 kg m^{-3} (Ren et al., 2004). The total mass change for RGs (ΔV_{RG}) was calculated by summing δV_{RG} at each 20 m altitude interval over all glacierized areas of RGs. Mass change uncertainties (U_{mc}) were calculated by applying the conventional error propagation procedure, i.e. $U_{mc} = \mathrm{Sqrt}(U_{\Delta h}^2 * \rho^2 + U_{\rho}^2 * \Delta h^2)$, where $U_{\Delta h}$ and U_{ρ} are uncertainties of glacier surface elevation change (Δh) and average glacier density (ρ).

The elevation-change uncertainty was estimated based on the averaged vertical differences and its standard deviation within each 20-m altitude interval in ice-free terrain (Table 2).

3.4. Hydrological and meteorological observations

At a site (86°57′E, 28°22′N; 4270 m a.s.l.) downstream of RR (Fig. 1), runoff was measured every day in April–November 2010, by the Qomolangma Atmospheric and Environmental Observation and Research Station, CAS (QOMORS).

Meteorological parameters were observed at Dingri meteorological station (DMS: 86°07′E, 28°40′N; 4300 m a.s.l., Fig. 1) from 1961 to 2010 (Table 3). According to the monthly mean temperatures at DMS, there are clear seasonal variations, with temperatures below 0 °C between November and March. Snow and ice melt may begin once the mean daily temperature remained above 0 °C since every April. The number of melting days in each year was counted for those days of positive mean daily air temperature and averaged by a decade, i.e. mean annual melting days (MD, Table 3).

The modeled actual evapotranspiration (ET_A, mm a^{-1}) was calculated by Yin et al. (2013) based on the modified Lund–Potsdam–Jena dynamic vegetation model (LPJ) and monthly meteorological data in spatial grids (resolution of 0.1° × 0.1°) from 1981 to 2010, which were interpolated from observations of 80 meteorological stations on TP by considering elevation effects using the thin plate spline method (Yin et al., 2013). Moreover, for RC, annual precipitation (P^*), modeled evapotranspiration (ET_A^*), and annual water balance ($P–E_A^*$) were derived at seven grids (resolution of 0.1° × 0.1°) from Yin et al. (2013) and they were averaged for each decade from 1981 to 2010 presented in Table 3.

The measured actual evapotranspiration (ET_a) was obtained from eddy covariance system at QOMORS since 2010, which was

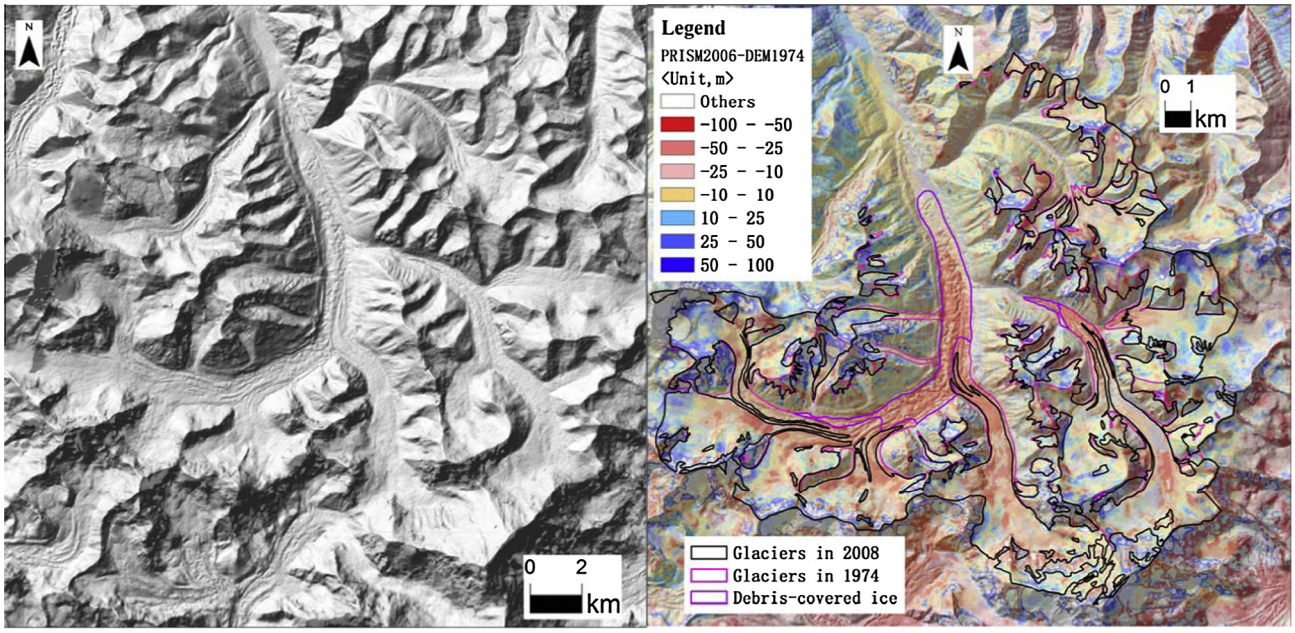

(a) Hillshade of the generated PRISM2006 by ALOS/PRISM data on 04 Dec 2006.

(b) Elevation differences (m) between 2006 and 1974.

Fig. 3. The generated PRISM2006 and its elevation difference to DEM1974. (a) Hillshade of the generated PRISM2006 by ALOS/PRISM data on 04 December 2006. (b) Elevation differences (m) between 2006 and 1974.

Table 2
Elevation difference (m) with respect to the base DEM1974 in the ice-free areas.

	PRISMV06	PRISM2006	PRISMV06*	PRISM2006*	PRISMV06**	PRISM2006**
Max	1441.66	144.53	99.99	100	51.83	51.83
Min	−548.91	−680.4	−100	−100	−24.31	−24.31
AVG	−1.43	0.01	−8.44	−8.18	−7.79	−7.57
STDEV	42.96	44.84	28.12	28.37	6.36	6.5
Uncertainty(m/a)	–	–	–	–	±0.23	±0.23

Note:
(1) PRISMV06, the generated PRISM DEM with gaps from ALOS/PRISM data on 04 December 2006.
(2) PRISM2006, was obtained by filling data gaps for PRISMV06.
* Grid cells with elevation differences exceeding ±100 m were omitted as outliers.
** Averaged by 20-m interval in altitude in the ice-free areas.

Table 3
Mean annual air temperature (T, °C), mean annual melting days (MD) at the Dingri meteorological station (DMS), annual precipitation (P, mm a^{-1}), modeled evapotranspiration (ET_A, mm a^{-1}), measured evapotranspiration (ET_a, mm a^{-1}) with the eddy covariance system and the mean annual water residual between P and E (P–ET_A, or P–ET_a, mm a^{-1}) at DMS and RC/QOMORS.

DMS						RC/QOMORS				
Time	T	MD	P	ET_A	P–ET_A	T	P^*	ET_A^*	ET_a	P–E^*
1960s	0.9	175	256			–	–	–	–	–
1970s	2.7	194	340			–	–	–	–	–
1980s	2.7	195	332	252	80	–	530	302	–	228
1990s	3.2	200	386	285	101	–	457	288	–	169
2000s	3.8	208	378	296	82	–	473	300	–	173
1981–2010	3.5	201	365	278	87		485	296	–	189
2008	3.8	207	446	342	104	3.3	147	308	–	
2009	4.3	216	265	235	30	4.4	113	283	–	
2010	4.2	228	440	288	152	4.2	304	307	300	4

Note:
(1) P^*, ET_A^* and P–E^* in 1980s, 1990s, 2000s, and 1981–2010, are the averaged spatial meteorological data for RC by 7 grid points with a resolution of 0.1° × 0.1° from Yin et al. (2013).
(2) All data in the lower right column are observed data at QOMORS in 2008-2011, except for the modeled ET_A.

considered as the most accurate way for accessing evapotranspiration data. Comparing ET_a with ET_A at QOMORS, it shows that the uncertainty of ET_A was within 10 mm a^{-1} (Table 3).

4. Results

4.1. Surface elevation changes with altitudes and surface conditions

The average elevation change of the entire glacier surfaces in RC was -0.47 ± 0.23 m a^{-1} during 1974–2006, which included the debris-covered tongues (Table 4). The exposed ice, including all visible debris-free glaciers and ice until the lower limit of sérac zone (Fig. 2b), showed an average elevation change of -0.40 ± 0.23 m a^{-1}.

Glacier elevation changes in RC are spatially variable and indicate a clear dependency on altitude (Figs. 4 and 5). Surface elevation changes in the debris-free glacier tongues at altitudes around 5360–5750 m a.s.l. are highly negative, with an average of -1.36 ± 0.23 m a^{-1} (Fig. 4a). Whereas, in the accumulation area, elevation changes are slightly positive in the highest part around 8500 m (Fig. 4a).

As clearly seen in Fig. 4b, elevation changes are largely negative in the debris-covered tongues, located at a lower altitude than the clean ice part. The average elevation change there was -1.37 ± 0.23 m a^{-1}. The zones of the maximum lowering are located in 5240–5740 m, being the transition zone between the active and inactive glaciers, where the elevation change is -1.61 ± 0.23 m a^{-1} (Fig. 4b). Over the debris-covered tongue around 5200–5760 m, widespread melting ponds (Fig. 2c) have developed on the stagnant ice and moraine-dammed lakes have formed. The supra-glacial lakes have grown in area and in numbers since the 1970s (Ye et al., 2009).

Table 4
Glacier mass changes at Rongbuk catchment in 1974–2006 with their uncertainty followed by ±.

Glacier name/type	Area (km^2)	Elevation change (m a^{-1})	Mean mass change (m a^{-1} w.e.)	Total mass change (Gt a−1)
The West RG	39.59	−0.50 ± 0.23	−0.42 ± 0.27	−0.02 ± 0.02
The Middle RG	20.19	−0.37 ± 0.23	−0.32 ± 0.27	−0.01 ± 0.01
The East RG	42.23	−0.28 ± 0.23	−0.24 ± 0.27	−0.01 ± 0.01
Deb. cov. ice*	10.74	−1.42 ± 0.23	–	−0.01 ± 0.003
Exposed ice	144.14	−0.40 ± 0.23	−0.34 ± 0.27	−0.05± 0.04
All ice in RC	155.62	−0.47 ± 0.23	−0.40 ± 0.27	−0.06 ± 0.04

* The Debris-covered ice.

Remarkable spatial differences in elevation change were found between the different branches (Fig. 5), being -0.50 ± 0.23 m a^{-1} for West, -0.37 ± 0.23 m a^{-1} for Middle, and -0.28 ± 0.23 m a^{-1} for East RG. Over the lower reaches (5680–5940 m) of the East RG, the overall elevation change was -30 ± 2.04 m in 1974–2006, which was very close to the in-situ GPR measurements of about −30 m along the main flow-line during 1974–2009. An average ice thickness in RG was about 190 m with a maximum about 320 m at 6300 m a.s.l. in 2009 (Zhang et al., 2012a,b).

It is difficult to identify the actual positions of glacier snouts on optical images due to thick debris covers. However, it seems that the RG snout might have been located around 5240–5260 m during the study period, considering the sharp surface lowering rate from there to the higher altitudes (Fig. 4b).

4.2. Mass changes in RC

The mass changes of glaciers in RC were clearly negative from 1974 to 2006 (Table 4). However, the changes were not homogeneous, varying with altitudes and among different glaciers. Vertical distributions of mass changes at RGs are shown in Fig. 5a–c, for the West, Middle and East RGs. We found a mass change of -0.05 ± 0.04 Gt a^{-1} for the exposed glacier ice, -0.01 ± 0.003 Gt a^{-1} for the debris-covered ice, and -0.06 ± 0.04 Gt a^{-1} in total. Thus, it was found that mass changes of glaciers showed strong spatial variations in RC.

5. Discussion

5.1. Glacier thinning and debris cover conditions

Glacier surface elevation change can be regarded as the ice thickness change, so far as the bedrock elevation is considered unchanged. A positive thickness change indicates thickening, and

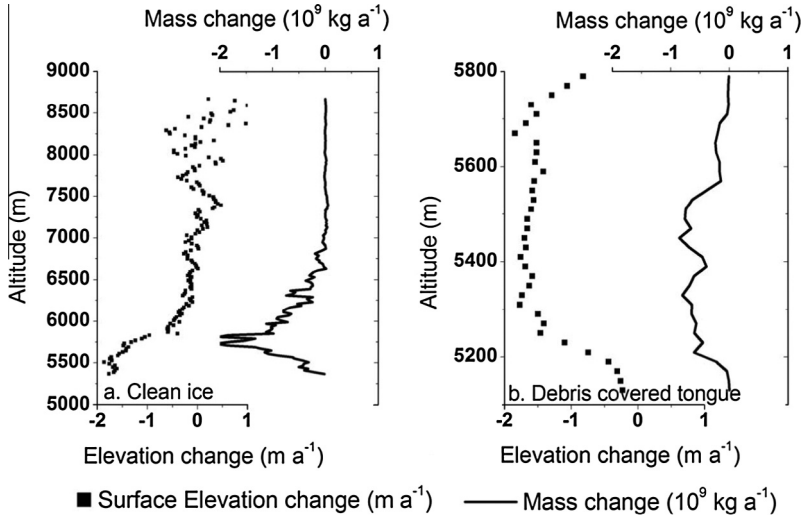

Fig. 4. Glacier elevation and ice mass changes at each 20 m interval by altitude in Rongbuk catchment for (a) the clean-ice and (b) the debris-covered parts for the period 1974–2006.

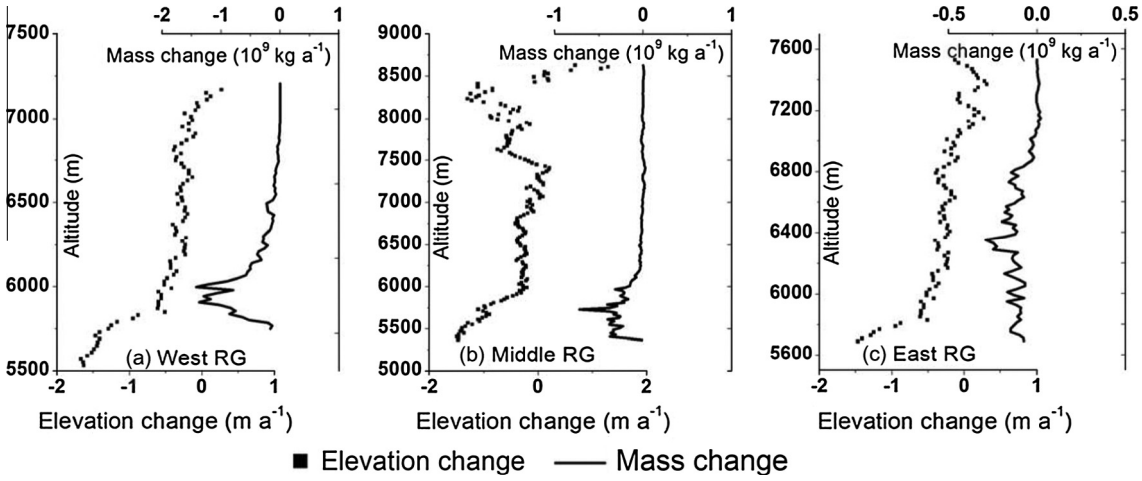

Fig. 5. Glacier elevation changes and ice mass change at each 20 m interval by altitude on three tributaries of Rongbuk Glaciers (RG) during 1974–2006.

negative indicates thinning of ice. Thickening or thinning at a point of a glacier is caused by an arithmetic sum of surface mass balance (snow accumulation and ice ablation) and emergence flow velocity caused by longitudinal compression of a glacier. When we consider a certain snout area of a glacier, such as a debris-covered region, the average thickness change in the area can be regarded as resulted from a sum of the total surface mass balance over the area and the total downstream inflow of ice through the cross section.

Interestingly, the debris-covered regions obviously exhibit higher thinning rates than the exposed ice regions on average (Fig. 4). It is known that ice ablation rate is highly reduced under the thick debris-cover due to the insulation effect of debris. However, the debris-covered regions are normally located in the lower altitudes, i.e. the higher temperature conditions. The development of supra-glacial lakes and the enhanced ice melting on the cliffs of them (Benn et al., 2012; Sakai and Fujita, 2010; Sakai et al., 2002) are probably one reason for the larger mass loss on the debris-covered tongue than on the clean-ice region.

In addition, it can also be considered that a decrease in ice flux due to becoming less active in glacier flow, as for example measured on glaciers south of MQ (Bolch et al., 2008; Quincey et al., 2009), may have caused the high thinning of the debris-covered tongue.

5.2. Glacier mass changes in the Himalayas

Results show that the average mass change in RGs was substantially negative as -0.40 ± 0.27 m a^{-1} w.e. in 1974–2006. Similar rates have also been found for adjacent glaciers and regions. Mass changes were obtained as -0.40 ± 0.25 m a^{-1} w.e. in 1992–2008 (Nuimura et al., 2012) and -0.32 ± 0.08 m a^{-1} w.e. in 1970–2007 (Bolch et al., 2011) both on the southern flank of MQ. Gardelle et al. (2013a) observed a mass change of -0.59 ± 0.16 m a^{-1} w.e. (2000–2011) for the north-flowing RG based on DEM differencing. Kääb et al. (2012) obtained a mass loss of -0.30 m a^{-1} w.e. in east Nepal and Bhutan Himalayas during 2003–2008 based on ICESat laser altimetry data. Neckel et al. (2014) reported an average mass change of -0.66 ± 0.32 m w.e. a^{-1} in 2003–2009 in the central and eastern Tibetan Himalaya using similar data.

Thus, as far as detailed studies were made, Himalayan glaciers have certainly lost mass during the last decades.

5.3. Possible climatic controls

Glacier and climate changes at MQ have been studied since the 1950s (Liu et al., 1962; Miller et al., 1965; TSETCAS, 1962). Melting of glaciers has resulted in the formation and expansion

of moraine-dammed lakes in the MQ (Sagamartha) region (Bajracharya and Mool, 2009; Bolch et al., 2008; Osti et al., 2011; Ye et al., 2009). It suggests that rising temperature is a major factor for glacier recessions in the Himalayas and for the increase in runoff from RC (e.g. Liu et al., 2010). Increased black carbon concentrations from an Everest ice core in 1975–2000 provides information about increased absorption of radiation that might also contribute to glacier melt enhancement (Kaspari et al., 2011). The weakening of the summer Indian monsoon has reduced local precipitation (Mölg et al., 2014; Yang et al., 2011) and decreased snow accumulation as e.g. found on the East RG (Kaspari et al., 2008).

Clearly recognized in Table 3 are a continuous accelerated rising trend of annual mean air temperature by 1.06 °C in the last three decades since the 1970s, a linearly increasing of number of melting days, and fluctuating water balance between annual precipitation and evaporation. Variations in these parameters, in addition to the rough terrain, may cause glacier mass changes in a complex heterogeneous manner.

5.4. Glacier contribution to the overall runoff

The mean annual P was larger than ET_A^* by about 189 mm a^{-1} in RC during a period of 1981–2010 (Table 3).

The annual runoff (R_0) in 2010 was estimated at about 0.28 km^3 a^{-1} (or runoff depth, R_d of 370 mm a^{-1} in the catchment area of 759 km^2) by summing up the daily runoff in observed days and assuming the minimum daily runoff as the base flow during a non-observed winter from December to March.

Although the runoff data at QOMORS are available only in 2010, if we simply assume that the 2010 data are more or less representative through the period of 1981–2010, the runoff from water balance P–E (189 mm) was roughly estimated as a half of the runoff depth R_d (370 mm a^{-1}). It is comparable with the result of in-situ investigations made near the outlet of RC (Fig. 1) in 1959–1960 by TSETCAS (1962). In a hydrological year from April 1959 to March 1960, runoff was observed as 0.15 km^3 a^{-1} (or 460 mm a^{-1} in the catchment area of 326 km^2), annual P and E was respectively observed as 335 mm a^{-1} and 129 mm a^{-1}. Then, water balance between P and E (206 mm a^{-1}) is considered to contribute to the runoff by about 45%.

The contribution of glaciers in RC, namely −0.06 km^3 a^{-1} w.e. (or runoff depth, R_g of 214 mm a^{-1} over an area 280 km^2) for the average total mass changes in 1974–2006, to the runoff in 2010 was found to be approximately 58%, i.e. $R_g/R_d \times 100\%$. Only for reference, if we use the runoff data (460 mm a^{-1}) in 1959–60, we obtain the glacier contribution of 47%. To summarize the above estimates, contributions to the runoff are 45–50% by P–E, 50% or more by glacier mass loss.

6. Conclusions

This study presented geodetically derived glacier surface elevation and mass change estimates in RC on the northern slope of the Central Himalayas. The results showed the suitability of using ALOS PRISM data for the generation of DEMs in high mountain regions with steep terrains. However, careful relative adjustments of the DEMs are necessary and there are still high uncertainties at the higher altitude with complex terrains and low optical contrast.

Obtained elevation changes of glaciers in RC indicate remarkable variability with location sites, altitudes, and the surface conditions. Particularly, elevation changes of the debris-covered ice are much higher than the exposed ice, which is considered to be related to the lower altitude location and developments of supra-glacial lakes on the debris-covered tongue.

Mass changes of glaciers in RC were derived as significantly negative in 1974–2006 (−0.40 ± 0.27 m a^{-1} w.e.), which is in tendency consistent with other glaciers in the Himalayas. Estimated total annual mass changes in RC were considered to contribute to about 50% or more of the total annual runoff from the catchment.

The other 45–50% of the runoff was estimated to be due to water balance between precipitation and evapotranspiration.

A continuous rising trend of annual mean air temperature (by 1.06 °C in 3 decades since the 1970s) and a linearly increasing of number of annual melting days were detected at the nearest meteorological station.

Acknowledgements

The research results have been obtained through the cooperation between the research organization (Institute of Tibetan Plateau Research, CAS) and JAXA (JAXA/METI for PALSAR) in JAXA's ALOS RA. The work is supported by the Special Basic Research Project of MST (2013FY111400-2), by NSF of China (41120114001, 41125003, 40971048, 41071254), by Foundation Program for outstanding Young Scholar of CAS (KZCX2-EW-QN104). The project was also supported by Open Research Fund of TEL in CAS, by Open Fund of State Key Laboratory of Remote Sensing Science and by in-situ investigated data from QOMORS. T.B. was funded by DFG (Codes: BO 3199/2-1 and BU 949/20-1) and ESA within the Glaciers_cci Project (4000101778/10/I-AM).

We would like to express our thanks to J.G. Cogley, G. Moholdt, R.L. Armstrong, L. Ying, B. Raup, W. Yang, A. Barrettand, F. Su, K. Tong, Y. Ma, Y. Zhang, W. Liu, C. Han and Y. Yin who provided instructive suggestions and useful meteorological data for the manuscript. We are also grateful to the anonymous reviewers, Konstantine P. Georgakakos, Ms. Pallavi Das, Dr. Ana Barros and C. Nuth whose help and comments were helpful for improvement of this paper.

References

Azam, M.F. et al., 2012. From balance to imbalance: a shift in the dynamic behaviour of Chhota Shigri Glacier (Western Himalaya, India). J. Glaciol. 58 (208), 315–324.

Bajracharya, S.R., Mool, P., 2009. Glaciers, glacial lakes and glacial lake outburst floods in the Mount Everest region, Nepal. Ann. Glaciol. 50 (53), 81–86.

Benn, D.I. et al., 2012. Response of debris-covered glaciers in the Mount Everest region to recent warming, and implications for outburst flood hazards. Earth-Sci. Rev.

Berthier, E. et al., 2007. Remote sensing estimates of glacier mass balances in the Himachal Pradesh (Western Himalaya, India). Remote Sens. Environ. 108 (3), 327–338.

Berthier, E., Schiefer, E., Clarke, G.K.C., Menounos, B., Remy, F., 2010. Contribution of Alaskan glaciers to sea-level rise derived from satellite imagery. Nat. Geosci. 3 (2), 92–95.

Bolch, T., Buchroithner, M.F., Peters, J., Baessler, M., Bajracharya, S., 2008. Identification of glacier motion and potentially dangerous glacial lakes in the Mt. Everest region/Nepal using spaceborne imagery. Nat. Hazards Earth Syst. Sci. 8 (6), 1329–1340.

Bolch, T. et al., 2012. The state and fate of Himalayan glaciers. Science 336, 310–314.

Bolch, T., Pieczonka, T., Benn, D.I., 2011. Multi-decadal mass loss of glaciers in the Everest area (Nepal Himalaya) derived from stereo imagery. Cryosphere 5 (2), 349–358.

Cogley, J.G., 2012. Climate science: Himalayan glaciers in the balance. Nature 488 (7412), 468–469.

Dobhal, D., Gergan, J., Thayyen, R.J., 2008. Mass balance studies of the Dokriani Glacier from 1992 to 2000, Garhwal Himalaya, India. Bull. Glaciol. Res. 25, 9–17.

Fujita, K., Nuimura, T., 2011. Spatially heterogeneous wastage of Himalayan glaciers. Proc. Natl. Acad. Sci. U.S.A. 108 (34), 14011–14014.

Fujita, K. et al., 2013. Potential flood volume of Himalayan glacial lakes. Nat. Hazards Earth Syst. Sci. 13, 1827–1839.

Gardelle, J., Berthier, E., Arnaud, Y., Kääb, A., 2013a. Region-wide glacier mass balances over the Pamir–Karakoram–Himalaya during 1999–2011. Cryosphere Discuss. (7), 975–1028

Gardelle, J., Berthier, E., Arnaud, Y., Kääb, A., 2013b. Region-wide glacier mass balances over the Pamir-Karakoram-Himalaya during 1999–2011. Cryosphere 7 (6), 1885–1886.

Gardner, A.S. et al., 2013. A reconciled estimate of glacier contributions to sea level rise: 2003 to 2009. Science 340 (6134), 852–857.
Holzer, N., Vijay, S., Yao, T., Xu, B., Buchroither, M., Bolch, T., 2015. Four decades of glacier variations at Muztag Ata (Eastern Pamir): a multi-sensor study including Hexagon KH-9 and Pléiades data. Cryosphere Discuss. 9, 1811–1856.
Huss, M., 2013. Density assumptions for converting geodetic glacier volume change to mass change. Cryosphere 7 (3), 877–887.
Immerzeel, W.W., Bierkens, M.F.P., 2010. Asian water towers: more on monsoons response. Science 330 (6004), 585–585.
Kääb, A., Berthier, E., Nuth, C., Gardelle, J., Arnaud, Y., 2012. Contrasting patterns of early twenty-first-century glacier mass change in the Himalayas. Nature 488 (7412), 495–498.
Kääb, A., Treichler, D., Nuth, C., Berthier, E., 2015. Brief communication: contending estimates of 2003–2008 glacier mass balance over the Pamir–Karakoram–Himalaya. The Cryosphere 9 (2), 557–564.
Kaser, G., Großhauser, M., Marzeion, B., 2010. Contribution potential of glaciers to water availability in different climate regimes. Proc. Natl. Acad. Sci. 107 (47), 20223–20227.
Kaspari, S. et al., 2008. Snow accumulation rate on Qomolangma (Mount Everest), Himalaya; synchroneity with sites across the Tibetan Plateau on 50–100 year timescales. J. Glaciol. 54 (185), 343–352.
Kaspari, S.D. et al., 2011. Recent increase in black carbon concentrations from a Mt. Everest ice core spanning 1860–2000 AD. Geophys. Res. Lett. 38.
Lei, Y.B. et al., 2012. Glacier mass loss induced the rapid growth of Linggo Co on the central Tibetan Plateau. J. Glaciol. 58 (207), 177–184.
Li, X. et al., 2008. Cryospheric change in China. Global Planet. Change 62 (3–4), 210–218.
Li, Z., Xing, Q., Liu, S., Zhou, J., Huang, L., 2012. Monitoring thickness and volume changes of the Dongkemadi Ice Field on the Qinghai-Tibetan Plateau (1969–2000) using Shuttle Radar Topography Mission and map data. Int. J. Digit. Earth 5 (6), 516–532.
Liu, W. et al., 2010. Hydrological Characteristics of the Rongbuk Glacier Catchment in Mt. Qomolangma Region in the Central Himalayas, China. J. Mt. Sci. 7 (2), 146–156.
Liu, Z., Liu, Z., Wang, F., 1962. Quaternary glacier developement comparison among Mt. Everest, Mt. Tengger, Mt. Qilian around Tuanjie peak. Acta Geographica Sinica 01, 19–33 (in Chinese).
Luedeling, E., Siebert, S., Buerkert, A., 2007. Filling the voids in the SRTM elevation model – a TIN-based delta surface approach. ISPRS J. Photogramm. Remote Sens. 62 (4), 283–294.
Ma, L., Tian, L., Pu, J., Wang, P., 2010. Recent area and ice volume change of Kangwure Glacier in the middle of Himalayas. Chin. Sci. Bull. 55 (20), 2088–2096.
Miller, M.M., Leventhal, J.S., Libby, W.F., 1965. Tritium in Mount Everest ice; annual glacier accumulation and climatology at great equatorial altitudes. J. Geophys. Res. 70 (16), 3885–3888.
Mölg, T., Maussion, F., Scherer, D., 2014. Mid-latitude westerlies as a driver of glacier variability in monsoonal High Asia. Nat. Clim. Change 4 (1), 68–73.
Neckel, N., Kropáček, J., Bolch, T., Hochschild, V., 2014. Glacier mass changes on the Tibetan Plateau 2003–2009 derived from ICESat laser altimetry measurements. Environ. Res. Lett. 9 (1), 014009.
Nuimura, T., Fujita, K., Yamaguchi, S., Sharma, R.R., 2012. Elevation changes of glaciers revealed by multitemporal digital elevation models calibrated by GPS survey in the Khumbu region, Nepal Himalaya, 1992–2008. J. Glaciol. 58, 648–656.
Nuth, C., Kääb, A., 2011. Co-registration and bias corrections of satellite elevation data sets for quantifying glacier thickness change. Cryosphere 5 (1), 271–290.
Osti, R., Bhattarai, T.N., Miyake, K., 2011. Causes of catastrophic failure of Tam Pokhari moraine dam in the Mt. Everest region. Nat. Hazards 58 (3), 1209–1223.
Paul, F., Haeberli, W., 2008. Spatial variability of glacier elevation changes in the Swiss Alps obtained from two digital elevation models. Geophys. Res. Lett. 35 (21).
Pieczonka, T., Bolch, T., Junfeng, W., Shiyin, L., 2013. Heterogeneous mass loss of glaciers in the Aksu-Tarim Catchment (Central Tien Shan) revealed by 1976 KH-9 Hexagon and 2009 SPOT-5 stereo imagery. Remote Sens. Environ. 130, 233–244.
Quincey, D.J., Luckman, A., Benn, D.I., 2009. Quantification of Everest region glacier velocities between 1992 and 2002, using satellite radar interferometry and feature tracking. J. Glaciol. 55 (192), 596–606.
Racoviteanu, A., Arnaud, Y., Williams, M., Manley, W.F., 2014. Spatial patterns in glacier area and elevation changes from 1962 to 2006 in the monsoon-influenced eastern Himalaya. Cryosphere Discuss. 8 (4), 3949–3998.
Ren, J., Qin, D., Kang, S., Hou, S., Pu, J., Jing, Z., 2004. Glacier variations and climate warming and drying in the central Himalayas. Chin. Sci. Bull. 49 (1), 65–69.
Sakai, A., Fujita, K., 2010. Formation conditions of supraglacial lakes on debris-covered glaciers in the Himalaya. J. Glaciol. 56 (195), 177–181.
Sakai, A., Nakawo, M., Fujita, K., 2002. Distribution characteristics and energy balance of ice cliffs on debris-covered glaciers, Nepal Himalaya. Arctic Antarct. Alpine Res. 34 (1), 12–19.
Shi, Y., Cheng, G., 1991. Cryosphere and global climate change. Bull. Chin. Acad. Sci. 6 (4), 287–291.
The Tibetan Scientific Expedition Team in Chinese Academy of Sciences (TSETCAS), 1962. Report of Scientific Expedition in Mt. Qomolangma Region. Science Press, Beijing.
The Tibetan Scientific Expedition Team in Chinese Academy of Sciences (TSETCAS), 1975. Report of Scientific Expedition in Mt. Qomolangma Region (1966-1968): Modern Glacier and Geomography. Science Press, Beijing.
Tian, L., Zong, J., Yao, T., et al., 2014. Direct measurement of glacier thinning on the southern Tibetan Plateau (Gurenhekou, Kangwure and Naimona'Nyi glaciers). J. Glaciol. 60 (223), 879–888.
Vincent, C. et al., 2013. Balanced conditions or slight mass gain of glaciers in the Lahaul and Spiti region (northern India, Himalaya) during the nineties preceded recent mass loss. The Cryosphere 7, 569–582.
Wang, P., Li, Z., Li, H., Wang, W., Yao, H., 2014. Comparison of glaciological and geodetic mass balance at Urumqi Glacier No. 1, Tian Shan, Central Asia. Global Planet. Change 114, 14–22.
Xie, Z.C., Su, Z., 1975. Glacier Development, Quantity and Distribution on the Northern Slope of Mt. Everest., Report of the 1966–1968 Scientific Expedition to the Qomoloangma Mountain (Mount Everest) Area, Recent Glaciology and Geomorphology. Science Press, Beijing, China (in Chinese), pp. 95–105.
Yang, W. et al., 2013. Mass balance of a maritime glacier on the southeast Tibetan Plateau and its climatic sensitivity. J. Geophys. Res.-Atmos. 118 (17), 9579–9594.
Yang, X., Zhang, T., Qin, D., Kang, S., Qin, X., 2011. Characteristics and Changes in Air Temperature and Glacier's Response on the North Slope of Mt. Qomolangma (Mt. Everest). Arctic Antarct. Alpine Res. 43 (1), 147–160.
Yao, T.D. et al., 2012. Different glacier status with atmospheric circulations in Tibetan Plateau and surroundings. Nat. Clim. Change 2 (9), 663–667.
Ye, Q.H. et al., 2009. Monitoring glacier and supra-glacier lakes from space in Mt. Qomolangma region of the Himalayas on the Tibetan Plateau in China. J. Mt. Sci. 6 (3), 211–220.
Yin, Y., Wu, S., Zhao, D., Zheng, D., Pan, T., 2013. Modeled effects of climate change on actual evapotranspiration in different eco-geographical regions in the Tibetan Plateau. J. Geophys. Sci. 23 (2), 195–207.
Zemp, M. et al., 2013. Reanalysing glacier mass balance measurement series. Cryosphere 7 (4).
Zhang, T., Xiao, C., Qin, X., Hou, D., Ding, M., 2012a. Ice thickness observation and landform study of East Rongbuk Glacer, Mt. Qomolangma. J. Glaciol. Geocryol. 34 (5), 1059–1066 (in Chinese with English abstract).
Zhang, Y., Liu, S., Shangguan, D., Li, J., Zhao, J., 2012b. Thinning and shrinkage of Laohugou No. 12 glacier in the Western Qilian Mountains, China, from 1957 to 2007. J. Mt. Sci. 9 (3), 343–350.